Damping of the Giant Resonance in Heavy Nuclei*

MICHAEL DANOS
National Bureau of Standards, Washington, D. C.

AND

WALTER GREINER†
Department of Physics and Astronomy, University of Maryland, College Park, Maryland

(Received 30 November 1964)

In heavy nuclei the damping of the giant resonance is due to thermalization of the energy rather than to direct emission of particles; the latter process is strongly inhibited by the angular-momentum barrier. The thermalization proceeds via inelastic collisions leading from the particle-hole state to two-particle–two-hole states. In heavy nuclei, several hundred such states are available at the energy of the giant dipole resonance. The rather large width of the giant resonance arises from the addition of many small partial widths of channels leading to the different two-particle–two-hole states. Both the density of the two-particle–two-hole states and the mean value of the interaction matrix elements between the particle-hole and two-particle–two-hole states are evaluated in a simplified square-well shell model. In a given nucleus the energy dependence of the widths is determined mainly by the density of states; the A dependence is determined mainly by the size of the matrix elements. For $A \approx 200$, we find $0.5\ \text{MeV} \leq \Gamma \leq 2.5\ \text{MeV}$. The uncertainty in this value comes mostly from the uncertainty in the strength of the interaction. Representing the energy dependence of the width by a power law we find for the exponent the value ~ 1.8.

I. INTRODUCTION

THE photodisintegration of heavy nuclei in the giant resonance proceeds in three steps. First, the incoming photon is absorbed and a collective nuclear motion is set up. Second, the energy of this coherent mode is dissipated into many degrees of freedom, i.e., the "mechanical" energy is transformed into "thermal" energy; the nucleus is being heated up. Third, the hot nucleus cools down by evaporating particles and photons. The first and the third of these steps has been treated quite extensively.[1–4] The investigation of the second step is the aim of this paper.

The damping of the collective state in heavy nuclei results from the excitation of complicated configurations. The direct emission of fast particles is here of minor importance owing to the angular-momentum barrier which limits the contribution of this process to the total width to about 10%. Because of the two-body character of the nuclear forces a complicated many-body configuration can be reached starting from the essentially particle-hole configuration of the collective state only by increasing the complexity of the state by adding *one* particle-hole excitation in each internal-scattering event.

After such an inelastic-scattering event, the coherence of the particle-hole state has been destroyed and there is no particular reason for any of the particles to recombine with any of the holes. In the coherent particle-hole state, the energy of the state is shifted by a considerable amount from the Hartree-Fock energy of a single particle-hole state; each particle-hole component of the coherent state is quite far off the energy shell. After the inelastic scattering, the state loses the coherence and the collective energy shift becomes available for distribution among the participating particles and holes. In this situation any final state in a following scattering event is as likely as any other, as long as the energy is approximately conserved in the event. Since, as will be shown below, there are several hundred states of this kind available it is extremely unlikely that the state will return to the coherent state. We calculate the process in the "they never come back" approximation where the lifetime of the coherent state is given by the probability that the first inelastic collision occurs.

The feature that the thermalization process of necessity has to go via the excitation of two-particle–two-hole states allows the latter states to be called "doorway states" in the terminology of Feshbach and Lemmer. One then could say that each particle-hole state has several hundred doors available through which to proceed to the thermal state.

The coherent state is supposed to be stationary as far as the collective excitations are concerned, i.e., it is obtained by coupling all collective modes.[3,5] The inelastic collisions then lead to states of noncollective character. Some of these second-generation states, and some of the states of later generations will contain low-angular-momentum neutrons of "thermal" energy which will be emitted as "evaporation" neutrons. In other words, they are damped and have finite widths. Therefore all states actually have some widths and do overlap. Thus,

* Research supported in part by the German Bundesministerium für Wissenschaftliche Forchung and the U. S. Office of Naval Research.

† Permanent address: University of Frankfurt, Frankfurt, Germany.

[1] G. Brown and M. Bolsterli, Phys. Rev. Letters 3, 472 (1959).

[2] V. Gillet, thesis, University of Paris, Rapport CEA 2177, Saclay, 1962 (unpublished). Many references are given in this paper.

[3] M. Danos and W. Greiner, Phys. Rev. 134, B284 (1964).

[4] J. M. Blatt and V. Weisskopf, *Theoretical Nuclear Physics* (John Wiley & Sons, New York, 1952), Chap. VIII.

[5] G. Ripka (private communication).

the transitions into the second-generation states can be treated like transitions into continuum states. The probability of this process is given by a formula which has the form of the "golden rule" of first-order perturbation theory. However, as we shall see, the formula is of much greater validity.

Previously this problem has been investigated in a few papers. Reifman[6] described the giant resonance in the independent-particle shell model and considered the damping to be due to the excitation of surface oscillations by the what now would be called particle-hole state. Neglecting configuration interactions he found a strong coupling between the particle-hole states anticipating in a certain sense the results of Danos and Greiner[3] on the coupling of dipole and surface collective states. The strength of this coupling implies however that it has to be treated more precisely by diagonalization and thus the surface states then are not available any more as a dissipative mechanism. Fujita[7] introduced the giant-resonance state by a coordinate transformation on the nucleon coordinates in the ground state and tried to determine the width of this state by the evaluation of certain commutators involving the nuclear Hamiltonian. The expressions yielded disappointingly large values for the width. The reason for this was that his method of calculation did not single out the dissipative part but gave the total spread of the dipole state over energy. In addition, the ground state used was not an eigenstate of the Hamiltonian but an independent particle state. The nonstationary character of this ground state also contributed to the width obtained.

Wildermuth[8] calculated the width of the giant resonance in the Fermi-gas model. The mechanism considered for the damping was essentially correct, namely, he considered the scattering of individual protons or neutrons which would lead to the destruction of the coherent state. He made some unjustified assumptions which, however, can be circumvented *a posteriori*. His Fermi-gas treatment also did not include the effects of correlations, i.e., the collective energy shift.

There exist several other papers which consider the width of the giant resonance to be due to the spread in energy of the independent-particle states. However, after diagonalization essentially only one dipole state remains[1,9] and the other states do not appear in the photon-absorption cross section, having lost their strength to the dipole state.

The damping of the giant-resonance modes in light nuclei, which results almost totally from penetration through the centrifugal barrier, has been calculated by Bauer and Ferrell[10] for the case of O^{16}. This damping mechanism gives only an unimportant contribution to the widths in heavy nuclei.

In Sec. II we shall describe in detail the various features of the damping mechanism and the approximations inherent in the method of calculation. The mathematical details of the problem are formulated in Sec. III. In Sec. IV we obtain the density of two-particle–two-hole states available for the damping process. We explicitly take into account energy and angular-momentum conservation. In Sec. V we obtain a value for the averaged matrix element in a simplified square-well model of the nucleus. Section VI gives the results and a discussion of the important parameters which enter the calculations. In Appendix A we give by means of time-dependent perturbation theory a simple derivation of the "golden rule" formula which we use in Secs. III, IV, V, and VI. In Appendix B we give a derivation of this formula which is formally exact in the nuclear Hamiltonian and of lowest order in the electromagnetic interaction. We demonstrate explicitly at which point a random-phase assumption enters, and furthermore, we also show that the photon-absorption line shape consists of a superposition of Lorentz rather than Breit-Wigner lines. In Appendix C we have collected some of the complicated expressions entering the density-of-states formulas of Sec. IV.

II. DESCRIPTION OF THE MODEL

All collective modes are essentially single-particle excitations, i.e., they are linear combinations of states which differ from the ground state in the state of one particle only. In the language in vogue at the present time, they are one-particle–one-hole states. This is necessarily so because they have large electromagnetic transition probabilities to the ground state and the transition operator is a sum of one-body operators. In terms of graphs they are thus represented essentially by single "sausages" which may go backward as well as forward (Fig. 1). In such chains each particle and its hole partner are coupled to the spin and parity of the particular collective state, i.e., 1^- for the dipole state, 2^+ for surface oscillations. It has been shown earlier[3] that some dipole and surface states are strongly coupled. Such a state would be depicted by graphs like Fig. 2. The configurations corresponding to the region of Fig. 2 where two sausages are present do not have multipole moments to the ground state. The transition strength of such a state is thus decreased and it reappears at the state corresponding to the excitation of a surface quan-

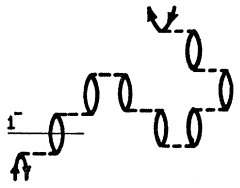

FIG. 1. Essential structure of a collective state.

[6] A. Reifman, Z. Naturforsh. **84**, 505 (1953).
[7] J. Fujita, Progr. Theoret. Phys. (Kyoto) **16**, 112 (1956).
[8] K. Wildermuth and H. Wittern, Z. Naturforsch. **12a**, 39 (1957).
[9] V. V. Balashov, V. G. Shevchenko, and N. P. Yudin, Nucl. Phys. **27**, 323 (1961).
[10] M. Bauer, University of Maryland Tech. Rept. 260, 1962 (unpublished); R. A. Ferrell, Bull. Am. Phys. Soc. **6**, 314 (1961).

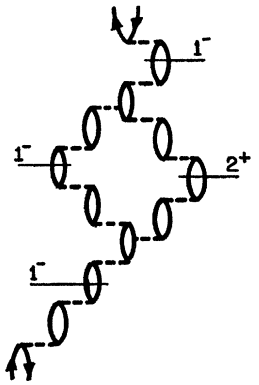

FIG. 2. Coupling of a dipole and a surface mode.

tum in addition to the dipole state which, as a matter of fact, is also represented by a graph of the form of Fig. 2.

In the consideration of the damping of the giant resonance we begin with a state which has been diagonalized with respect to the collective modes. Because of the configuration interaction the energy of the state differs from the sum of the energies of the participating particles and holes by about 5 to 10 MeV; we limit ourselves here to heavy nuclei. The high-energy particles of the dipole particle-hole state have mostly large angular momenta.[9,11] Their emission therefore is strongly inhibited by the centrifugal barrier

$$\frac{\hbar^2}{2M}\frac{l(l+1)}{r^2}=21\text{ MeV}\frac{l(l+1)}{r^2},\quad r\text{ in }10^{-13}\text{ cm}\qquad(1)$$

which shows that even at the top of the energy spectrum the neutron energy is about 8 to 10 MeV below the barrier height. The resulting penetrability is thus considerably smaller than $\frac{1}{10}$. Except for closed-neutron-shell nuclei, the "direct" emission of the excited particle leaves the hole buried below the Fermi surface, i.e., the nucleus is left in an excited state thus reducing the available energy for the outgoing neutron which results in a further decrease of the penetrability. The penetrability of the protons is still much smaller owing to the additional Coulomb barrier. The damping of the giant resonance thus cannot be due to the direct emission of particles. This is in agreement with experiment which indicates that only about 10 percent of the emitted particles are prompt; the overwhelming majority consists of evaporation neutrons.

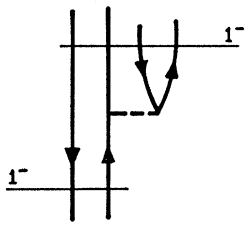

FIG. 3. The basic diagram for the thermalization of the energy. After the collision the coherence of the dipole state is gone. Angular momentum is conserved only for the total excitation.

[11] D. H. Wilkinson, Physica 22, 1039 (1956).

We now turn to the details of the thermalization process. The beginning of the thermalization is given by the inelastic scattering of the particle or the hole (see Fig. 3) with the excitation of a state other than a collective state. After the collision no particle-hole pair is separately coupled to 1^-; only the total state of two particles and two holes is coupled to 1^-, in contradistinction to the case of mixing collective states, illustrated in Fig. 2. Furthermore, after the scattering the particle will find itself in arbitrary states; i.e., states other than the configurations participating in the dipole state can and will be populated. Thus after the collision the collective energy shift must be accommodated by the particle and hole excitations; the states must return to the energy shell. This is, in fact, an important consideration; it shifts the nucleus to a region of higher level density. After this first collision any further scattering process is *a priori* as likely as any other as long as the energy is approximately conserved. Because of the large number of available states the probability is overwhelming that a "cascade" develops at this point. Ultimately a low-angular-momentum neutron state of sufficient energy will be excited which then will enable the neutron to escape (Fig. 4).

The last part of the process, viz., the escape of "thermal" neutrons, is very important. In the absence of such a possibility the process of Fig. 3 would not lead to damping of the collective state but would instead just produce a fine structure, a splitting of the state into many sharp levels. Qualitatively this can be explained most easily in terms of a classical picture. Consider a system of coupled oscillators. If one of them is suddenly excited the energy will not remain localized at this one oscillator but "beats" will set in, transferring the energy away from this "struck" oscillator. According to Liouville's theorem the energy will after certain time intervals more or less completely return to the struck oscillator, and a Fourier analysis would reveal just a certain number of discrete lines, viz., the normal-mode frequencies. The situation changes radically if some of the oscillators are damped. Now essentially *all* normal modes will be broadened, and beginning from a certain magnitude of this damping, the levels will coalesce. The energy then will be dissipated before the elapse of the "Poincaré time" and the struck oscillator will not start moving again once the energy has left it the first time. In other words, the damping of the system must be sufficient only to dissipate the energy during the Poincaré time which is determined by the number of coupled oscillators, a measure of which is the separation of the normal-mode frequencies. Only under these circumstances does the coupling to other oscillators lead to damping and not to splitting of the resonance. Then the width of the struck oscillator resonance is given by the "beat frequency," by the strength of the coupling to the other oscillators. In quantum-mechanical parlance this means that for damping to occur it is necessary that

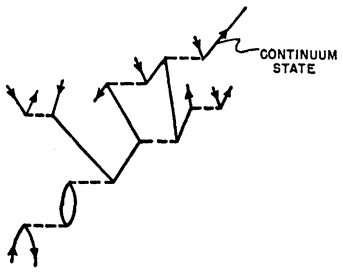

FIG. 4. Emission of a "thermal" neutron: After some "generations" a neutron of sufficiently low angular momentum and sufficiently high energy escapes leaving the nucleus behind in a possibly quite complicated state of medium excitation energy.

some of the participating states must be continuum states but it is sufficient that there exist very few such states. They also may lie a few generations away, i.e., a situation like that shown in Fig. 4 may obtain. However, already in the first generation some of the states may be escape states.

After the first inelastic collision has taken place and the state is on-the-energy shell the next collision will most of the time lead to more complicated configurations and the "return collision" (Fig. 5) has to compete on equal footing with all the other possibilities. Since there are of the order of hundreds of states available at this energy the they-never-come-back approximation is excellent and then, since the states actually are broadened and overlap, one can use the golden rule formula to calculate the lifetime of the dipole state. This point is discussed in detail in Appendices A and B. We re-emphasize here again that this procedure is applicable only because of the eventual evaporation of neutrons and the broadening of the many states which otherwise would be stationary and sharp. In the absence of neutron evaporation the golden rule calculation would actually be inapplicable. The "width" one would obtain when using it formally would just indicate the energy range over which the dipole state is distributed; this would not mean a damping of the state.

The many first-generation states must each be broadened only by a very small amount. It is just necessary that their width be large compared to the level spacing. Furthermore, each state may be coupled quite weakly to the dipole state. As it turns out, this actually is the case. The large width of the dipole state is thus not a consequence of a single strong process, but results instead from the combined effect of a large number of processes involving only weak coupling between each individual second-generation state and the dipole state.

A further very important point concerns the interference between the different possible graphs of the kind of Fig. 4. We shall make the explicit assumption that their contributions can be added incoherently. We believe that this assumption is eminently justified owing to the exceedingly large number of final states, i.e., excited states in which the nucleus is left after emission of a thermal neutron, and, in addition, owing to the very large number of quite diverse graphs participating in the process which assures randomness in the phases.

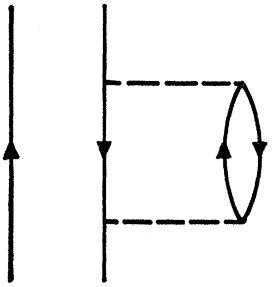

FIG. 5. Return collision: After the first scattering event the next collision can restore the dipole state. This process must compete with all other scattering possibilities.

Instead of using the golden rule one could calculate just the forward-scattering amplitude, e.g., in the single-collision approximation, Fig. 5, since it contains all the necessary information. We prefer, however, the more elementary approach for reasons of simplicity.

III. MATHEMATICAL FORMULATION OF THE PROBLEM

If $\Psi_u^{(1)}$ and $\Psi_v^{(2)}$ denote the one-particle–one-hole and the two-particle–two-hole states, respectively, and u, v are the appropriate quantum numbers, we have

$$\Psi_u^{(1)}=\sum_{\mu_1\mu_2}\langle f_1\mu_1 f_2\mu_2|1\tau_1\rangle a_{f_1\mu_1}{}^\dagger b_{f_2\mu_2}{}^\dagger|0\rangle, \quad (2)$$
$$u=\{f_1 f_2 1\tau_1 k_1 k_2\},$$

$$\Psi_v^{(2)}=Z\sum_{\nu_1\nu_2\nu_3\nu_4 ab}\langle l_1 m_1 l_2 m_2|Aa\rangle\langle Aal_3 m_3|Bb\rangle \times\langle Bbl_4 m_4|1\tau_1\rangle a_{l_1 m_1}{}^\dagger b_{l_2 m_2}{}^\dagger a_{l_3 m_3}{}^\dagger b_{l_4 m_4}{}^\dagger|0\rangle, \quad (3)$$
$$v=\{l_1 l_2 l_3 l_4 AB1\tau_1 k_1 k_2 k_3 k_4\},$$

where $a_{lm}{}^\dagger$, $b_{lm}{}^\dagger$ are creation operators for particles and holes with angular momentum lm. f_1 and f_2 are the angular momenta of the one-particle–one-hole configuration. A and B are intermediate angular momenta of the two-particle–two-hole state. Different A, B and the same l_1, l_2, l_3, l_4 are different two-particle–two-hole configurations. The wave numbers (energies) of the single-particle states are denoted by k. Z is a normalization factor, which can easily be calculated to be

$$Z=\Bigg\{1+(2A+1)(2B+1)\times\Bigg[\begin{Bmatrix}A & l_1 & l_2\\ l_3 & A & B\\ B & l_2 & 1\end{Bmatrix}\delta_{l_2,l_4}-\begin{Bmatrix}l_2 & l_1 & A\\ A & 1 & B\end{Bmatrix}^2\delta_{l_1,l_3}\delta_{l_2,l_4}\Bigg]-\frac{2A+1}{2B+1}\begin{Bmatrix}l_1 & l_2 & A\\ l_1 & B & A\end{Bmatrix}\delta_{l_1 l_3}\Bigg\}^{-1/2}. \quad (4)$$

The matrix element of the residual nuclear force is

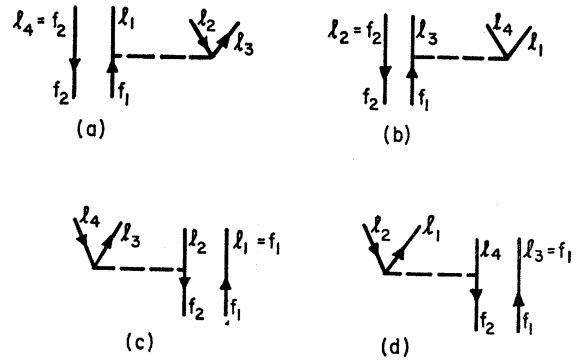

FIG. 6. Graphs of Eq. (7). The first two graphs, (a) and (b) describe the scattering of the particle. The second two graphs, (c) and (d) describe the hole scattering.

given in general in terms of particle creation and annihilation operators by

$$V=\tfrac{1}{2}\sum V_{\alpha\beta;\gamma\delta}a_\alpha{}^\dagger a_\beta{}^\dagger a_\gamma a_\delta. \tag{5}$$

We introduce in the usual way the hole operators for the states λ below the Fermi surface

$$\begin{aligned} a_\lambda{}^\dagger&=(-)^{l_\lambda-m_\lambda}b_{-\lambda},\\ a_\lambda&=(-)^{l_\lambda-m_\lambda}b_{-\lambda}{}^\dagger, \end{aligned} \tag{6}$$

where we have used the phase convention of Bell.[12] We notice that the following terms of (5) give contributions to the matrix elements $\langle\Psi^{(1)}|V|\Psi^{(2)}\rangle$

$$\begin{aligned}\langle\Psi^{(1)}|V|\Psi^{(2)}\rangle=&\tfrac{1}{2}\sum V_{\alpha\beta,\gamma\delta}\\ &\times[(-)^{l_\beta-m_\beta}a_\alpha{}^\dagger b_{-\beta}a_\gamma a_\delta+(-)^{l_\alpha-m_\alpha}b_{-\alpha}a_\beta{}^\dagger a_\gamma a_\delta\\ &+(-)^{l_\alpha-m_\alpha+l_\beta-m_\beta+l_\gamma-m_\gamma}b_{-\alpha}b_{-\beta}b_{-\gamma}{}^\dagger a_\delta\\ &+(-)^{l_\alpha-m_\alpha+l_\beta-m_\beta+l_\delta-m_\delta}b_{-\alpha}b_{-\beta}a_\gamma b_{-\delta}{}^\dagger]. \end{aligned} \tag{7}$$

The different processes occurring in (7) are represented by the graphs of Fig. 6. Each of these graphs, together with its exchange form, describes a different process. In (a) and (b) the hole "lies at rest" and the particle is scattered and creates a new particle-hole pair. In process (c) and (d) the particle is unaffected and the hole scatters and creates a particle-hole pair. In fact, the graphs (a) and (b) cover almost the same function space, albeit in a different coupling scheme (representation). The direct and exchange terms of the graphs of Fig. 6 are

$$\begin{aligned} &\text{(a)}\quad \delta_{f_2l_4}\delta_{\nu m_4}[V_{f_1l_2,l_1l_3}-V_{f_1l_2,l_3l_1}](-)^{l_2-m_2},\\ &\text{(b)}\quad \delta_{f_2l_2}\delta_{\nu m_2}[V_{f_1l_4,l_3l_1}-V_{f_1l_4,l_1l_3}](-)^{l_4-m_4},\\ &\text{(c)}\quad \delta_{f_1l_1}\delta_{\mu m_1}[V_{l_2l_4,f_2l_3}-V_{l_4l_2,f_2l_3}]\times(-)^{l_2+l_4+f_2-m_2-m_4-\nu},\\ &\text{(d)}\quad \delta_{f_1l_3}\delta_{\mu m_3}[V_{l_4l_2,f_2l_1}-V_{l_2l_4,f_2l_1}](-)^{l_4+l_2+f_2-m_2-m_4-\nu}. \end{aligned} \tag{8}$$

If the force $V(1,2)$ is expanded in spherical harmonics

$$V(1,2)=\textstyle\sum_{LM}v_L(1,2)Y_{LM}{}^*(1)Y_{LM}(2), \tag{9}$$

the matrix element $V_{f_1l_2,l_3l_1}$, for example, is explicitly

$$\begin{aligned} V_{f_1l_2,l_3l_1}=&\textstyle\sum_{LM}\langle R_{f_1}(1)Y_{f_1\mu_1}(1)R_{l_2}(2)Y_{l_2m_2}(2)|v_L(12)Y_{LM}{}^*(1)Y_{LM}(2)|R_{l_3}(1)Y_{l_3m_3}(1)R_{l_1}(2)Y_{l_1m_1}(2)\rangle\\ =&\textstyle\sum_{LM}(-)^{L-M}\langle l_3m_3L-M|f_1\mu_1\rangle\langle l_1m_1LM|l_2m_2\rangle\langle l_3\|L\|f_1\rangle\langle l_1\|L\|l_2\rangle R_{f_1l_2,l_3l_1}(L), \end{aligned} \tag{10}$$

where

$$\langle a\|L\|b\rangle=\left[\frac{(2a+1)(2L+1)}{4\pi(2b+1)}\right]^{1/2}\langle a0L0|b0\rangle \tag{11}$$

are the reduced matrix elements and

$$R_{f_1l_2l_3l_1}(L)=\int R_{f_1}(1)R_{l_2}(2)R_{l_3}(1)R_{l_1}(2)v_L(1,2)r_1{}^2r_2{}^2dr_1dr_2. \tag{12}$$

R_l are the radial wave functions and l is here understood to represent all quantum numbers.

We now specialize to δ-function forces. Introducing the expressions (10) into (8) one can calculate by straightforward methods the matrix elements between the properly angular momentum coupled states (2), (3). We list the result for the graphs (a) and (b), exchange terms included:

$$\begin{aligned}\langle\Psi_u{}^{(1)}|V^{(a)}|\Psi_v{}^{(2)}\rangle=&(-)^{l_3+l_3+f_1}\frac{Z}{4\pi}\left\{\left[\frac{(2l_2+1)(2l_3+1)(2l_1+1)}{(2A+1)^2(2f_1+1)}\right]^{1/2}\right.\\ &\left.-(-)^{f_1}\left[\frac{(2l_1+1)(2l_2+1)(2l_3+1)}{(2f_1+1)^3}\right]^{1/2}\right\}\langle l_1l_20l_2|A0\rangle\langle A0l_30|f_10\rangle R_{f_1l_2,l_3l_1}\delta_{f_1B}\delta_{l_4f_2}, \end{aligned} \tag{13}$$

$$\begin{aligned}\langle\Psi_u{}^{(1)}|V^{(b)}|\Psi_v{}^{(2)}\rangle=&\frac{Z}{4\pi}[(2A+1)(2B+1)(2l_3+1)]^{1/2}R_{f_1l_4,l_3l_1}\sum_L\left\{(-)^{f_2+A+l_1}\langle l_1l_0L0|f_10\rangle\langle l_30L0|l_40\rangle\right.\\ &\left.\times\begin{Bmatrix}1&f_2&f_1\\ l_1&L&A\end{Bmatrix}\begin{Bmatrix}l_4&l_3&L\\ A&1&B\end{Bmatrix}-(-)^{f_1}(2L+1)\langle l_30L0|f_10\rangle\langle l_10L0|l_40\rangle\begin{Bmatrix}f_1&f_2&1\\ l_3&A&B\\ L&l_1&l_4\end{Bmatrix}\right\}\delta_{l_2f_2}. \end{aligned} \tag{14}$$

[12] J. S. Bell, Nucl. Phys. 12, 117 (1958).

Here

$$V=V_0\delta(\mathbf{r}_1-\mathbf{r}_2)$$

$$=V_0\frac{\delta(r_1-r_2)}{r_1r_2}\sum_{LM}Y_{LM}{}^{(1)}Y_{L-M}{}^{(2)}(-)^M \quad (15)$$

and

$$R_{f_1l_2;l_3l_4}\equiv\int R_{f_1}R_{l_4}R_{l_3}R_{l_1}r^2dr. \quad (16)$$

One can similarly derive expressions for the contributions due to the graphs (c) and (d), but we will not need the exact values of these for our estimate. Note, that the value of B is restricted: In the case (a) we have $B=f_1$; in all other cases B can have only the values $B=l_4+1$, l_4, l_4-1. Note also that the different graphs in Fig. 6 represent transitions to different coupling schemes of the final states. The difference between (a) and (b), for example, is that in (a) the value for $l_4=f_2$ and in (b) the value for $l_2=f_2$.

The width of the particle-hole state $\Psi_u{}^{(1)}$ is given by

$$\Gamma=\hbar T, \quad (17)$$

where the transition probability T for the transition from $\Psi_u{}^{(1)}$ to all $\Psi_v{}^{(2)}$ can be calculated by perturbation theory. (See Appendix A.)

$$\Gamma=2\pi\sum_v|\langle\Psi_u{}^{(1)}|V|\Psi_v{}^{(2)}\rangle|^2\frac{\gamma_v/2\pi}{(E-E_v)^2+\gamma_v{}^2/4}. \quad (18)$$

Here E is the energy of the giant resonance, E_v and γ_v are the energy and width of the two-particle–two-hole state $\Psi_v{}^{(2)}$. The sum goes over all two-particle–two-hole states with the same energy and total angular momentum as the particle-hole configuration, i.e., 1^-. Equation (18) could be calculated numerically exactly in an actual model for the single-particle states (for example, the oscillator model). Instead, we wish to obtain a formula which exhibits, at least approximately, the energy dependence of (18). We do this by replacing the summation in (18) by an integration and by introducing suitable average values and obtain

$$\Gamma=2\pi(|\langle\Psi_u{}^{(1)}|V|\Psi_v{}^{(2)}\rangle|^2)_{\mathrm{av}}\rho(E), \quad (19)$$

where $\rho(E)$ is the density of two-particle–two-hole configurations at the energy E which can be reached from the particular particle-hole state by a two-body collision.

Strictly speaking, (19) together with (18) is the defining equation for the averaged squared matrix element. However, with the usual assumption of randomness the mean value can be calculated separately. We expect that the average matrix element should be a very weak function of the energy; it may decrease very slowly with increasing energy. The energy dependence of Γ thus is given by $\rho(E)$. We now proceed to evaluate it.

IV. THE DENSITY OF TWO-PARTICLE–TWO-HOLE STATES

We choose for the model, in which we calculate the wave functions and the number of final states, the infinite square-well model. If the radius of the square-well potential is R, then the solutions of the Schrödinger equation in this potential are of the form

$$\varphi_{lm\nu}=j_l(k_\nu r)Y_{lm} \quad (20)$$

and the above numbers k_ν are given by the boundary condition

$$j_l(k_\nu R)=0. \quad (21)$$

For a given upper bound of the energy (i.e., of k) the condition (21) can be satisfied only for angular momenta $l\leq l_m$, where l_m is given by the condition that the first zero of the spherical Bessel function $j_{l_m}(kR)$ lies at the boundary R. We replace the $j_{l_m}(kr)$ by their asymptotic expressions

$$j_l(kr)\propto(kr)^{-1}\cos[kr-\tfrac{1}{2}(l+1)\pi] \quad (22)$$

and find for the first zero the equation

$$kr-\tfrac{1}{2}(l+1)\pi=\tfrac{1}{2}\pi,$$

which gives (K is the Fermi momentum)

$$l_m=(2KR/\pi)-2. \quad (23)$$

This estimate is numerically very accurate. Thus the number of states for a given l and given fixed energy is

$$n_l=(KR/\pi)-\tfrac{1}{2}l. \quad (24)$$

Since the $(2l+1)$ different states of the magnetic quantum number in (20) are degenerate, the total number of possible single-particle states in our system up to an energy K is

$$n(K)=\sum_{l=0}^{l_m}n_l(2l+1)=(4/3)(KR/\pi)^3+(KR/\pi)^2-(11/6)(KR/\pi)+\tfrac{1}{2}. \quad (25)$$

Using this expression one can determine the Fermi momentum from the equation

$$n(K)=\tfrac{1}{2}Z,\ \tfrac{1}{2}N \quad (26)$$

for protons and neutrons. The factor $\frac{1}{2}$ comes from the spin. The function $n(KR)$ is plotted in Fig. 7.

We introduce the density of states of given angular momentum by

$$\rho_l(K)=dn_l(K)/dK=R/\pi. \quad (27)$$

Note, that we do not count the m degeneracy of the state K, l, m in (27), because conservation of the z component of angular momentum allows only definite values of it in the matrix elements of (18).

Let us now count the number of states which contribute to the processes of graph (a) of Fig. 6 taking

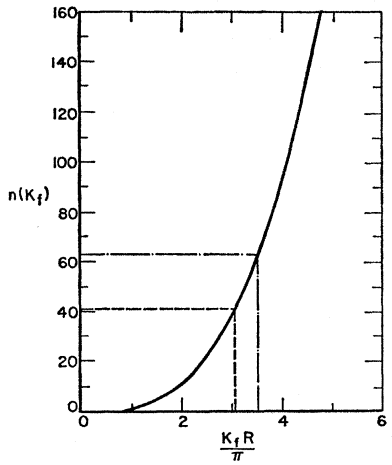

FIG. 7. Averaged number of states in a square well.

into account angular momentum and energy conservation. For the other graphs the considerations are similar and we will estimate the number of contributing states to the other four graphs later.

Because of $l_4=f_2$ and $B=f_1$, the angular momenta $l_1l_2l_3f_1$ have to fulfill the triangular rule

$$\Delta(l_1l_2l_3f_1)$$
$$=1 \text{ if } l_1,\ l_2,\ l_3,\ f_1 \text{ can be coupled to zero}$$
$$=0 \text{ if } l_1,\ l_2,\ l_3,\ f_1 \text{ cannot be coupled to zero.} \quad (28)$$

Energy conservation gives the condition

$$k_1^2+k_3^2-k_4^2=\kappa^2, \quad (29)$$

where $\hbar^2\kappa^2/2M$ is the energy of the particle-hole state, i.e., the giant-resonance energy. It is therefore fixed.

The number of final states fulfilling the conservation conditions (38), (29) is therefore

$$N(\kappa^2)=\sum_{l_1}^{l_m}\sum_{l_2}^{l_f}\sum_{l_3}^{l_m}\Delta(l_1l_2l_3f_1)$$
$$\times\int_{p_2}^{k_f}\int_{p_3}^{P_3}\int_{p_1}^{P_1}\rho_{l_1}(k_1)\rho_{l_2}(k_2)\rho_{l_3}(k_3)dk_1dk_2dk_3. \quad (30)$$

The upper limit of the momentum integrals is given by the condition (29) and the fact that the hole momentum k_2 can be maximally the Fermi momentum K:

$$P_1=(\kappa^2+k_4^2+k_2^2-k_3^2)^{1/2};\quad P_3=(\kappa^2+k_4^2+k_2^2)^{1/2}. \quad (31)$$

The lower limits are

$$\begin{aligned} p_1&=(l_1\pi/2R) && \text{if } (l_1\pi/2R)\geq K\\ &=K && \text{if } (l_1\pi/2R)\leq K;\\ p_2&=(l_2\pi/2R) && \text{if } (l_2\pi/2R)\leq K\\ &=K && \text{if } (l_2\pi/2R)\geq K;\\ p_3&=(l_3\pi/2R) && \text{if } (l_3\pi/2R)\geq K\\ &=K && \text{if } (l_3\pi/2R)\leq K. \end{aligned} \quad (32)$$

They exhibit the fact that the particle momentum has to be above the Fermi surface and the hole momentum has to be below the Fermi surface. Further, a given angular momentum can occur only above a certain minimum momentum given by $(l\pi/2R)$ [see (24)] and by the Fermi angular momentum for the hole.

Equation (30) is exact within our approximations. The integrals can be easily performed and we obtain

$$N(\kappa^2)=(R^3/\pi^3)\textstyle\sum_{l_1l_2l_3}\Delta(l_1l_2l_3f_1)\Big\{(\pi/4)(\kappa^2+k_4^2)(K-p_2)+(\pi/12)(K^3-p_2^3)$$
$$-\tfrac{1}{2}(\kappa^2+k_4^2)\int_{p_2}^{k_f}\arcsin\frac{p_3}{(\kappa^2+k_4^2+k_2^2)^{1/2}}dk_2-\frac{1}{2}\int_{p_2}^{k_f}k_2^2\arcsin\frac{p_3}{(\kappa^2+k_4^2+k_2^2)^{1/2}}dk_2$$
$$+p_1p_3(K-p_2)-(p_3K/4)(\kappa^2+k_4^2-p_3^2+K^2)^{1/2}+(p_3p_2/4)(\kappa^2+k_4^2-p_3^2+p_2^2)^{1/2}$$
$$-(p_3/4)(\kappa^2+k_4^2-p_3^2)\ln\frac{K+(\kappa^2+k_4^2-p_3^2+K^2)^{1/2}}{p_2+(\kappa^2+k_4^2-p_3^2+p_2^2)^{1/2}}-\tfrac{1}{2}pK(\kappa^2+k_4^2+K^2)^{1/2}$$
$$+\tfrac{1}{2}p_1p_2(\kappa^2+k_4^2-p_3^2)^{1/2}-\tfrac{1}{2}(\kappa^2+k_4^2)p_1\ln\frac{K+(\kappa^2+K^2+k_4^2)^{1/2}}{p_2+(\kappa^2+K^2+k_4^2)^{1/2}}\Big\}. \quad (33)$$

The expression in the braces depends via the $p_1p_2p_3$ in a complicated way on the l_1, l_2, l_3, Eq. (32). It is obvious that one cannot perform this sum exactly. We can proceed and we will obtain a good approximation, if we replace the p_ν by suitable mean values: The momenta p_1,p_3 lie above the Fermi surface and below $(K^2+\kappa^2)^{1/2}$. Suitable mean values for these are therefore

$$\bar{p}_1=\bar{p}_3=(K^2+\alpha\kappa^2)^{1/2}, \quad (34)$$

where α is a coefficient of the order $\alpha\approx\frac{1}{10}$. We will show later that the result does depend only very weakly on the choice of α. The momentum p_2 lies between 0 and K.

We expect physically that the largest contributions of holes in the two-particle–two-hole state will come from the region near the Fermi surface. We replace therefore

$$\tilde{p}_2 \approx k_4. \tag{35}$$

Now the expression in the braces is independent of l_1, l_2, l_3 and the sum can be performed. Before we do this, however, we simplify the complicated expression in the braces in the following way: When the particle-hole energy is zero ($\kappa^2=0$) then $k_4=K$. On the other hand, as the particle-hole energy increases, the holes lie progressively deeper below the Fermi surface. We therefore make the ansatz

$$k_4{}^2=k^2-\beta\kappa^2, \tag{36}$$

and β will be a coefficient of the order $\beta\approx\frac{1}{10}$. It can be determined accurately from the experimental positions of the hole in the giant resonance (remember, $\hbar^2k_4{}^2/2M$ = hole energy of the p-h state). Inserting (34), (35), and (36) into the complicated expression (33) for the braces and developing this expression in the small parameter $\kappa^2/K^2\approx\frac{1}{4}$ up to quadratic terms, we obtain after a straightforward, but lengthy calculation

$$N(\kappa^2)=(KR/\pi)^3[P(\kappa/K)^2+Q(\kappa/K)^4+\cdots]+\sum_{l_1l_2l_3}\Delta(l_1l_2l_3f_1), \tag{37}$$

where

$$\begin{aligned} P&=0.22\beta+0.031\alpha,\\ Q&=0.21\beta-0.089\alpha+0.045\alpha\beta-0.096\beta^2+0.049\alpha^2. \end{aligned} \tag{38}$$

P and Q are pure numbers depending only on the parameters α and β. We see however, that they depend mostly on β and weakly (especially P) on α. Therefore our averaging method is quite justified and the number of states we obtain with (37) should be a very good approximation.

We now determine the number of states compatible with angular-momentum conservation. That means, we count the number of nonvanishing Δ's in (37). We do it in the following way. We first introduce partial sums by

$$\sum_{l_1l_2l_3}\Delta(l_1l_2l_3f_1)=\sum_{l}^{l_f}F_v(l_mf_1l), \quad v=1,2, \tag{39a}$$

where

$$F_v(l_mf_1l)=\sum_{l_1l_3}\Delta(l_1l_2l_3f_1), \tag{39b}$$

with the constraint of triangularity between l_2, f_1, and l, i.e., $\mathbf{l}=\mathbf{l}_2+\mathbf{f}_1$. Thus l can have the value $|f_1-l_2|\leq l\leq|f_1+l_2|$. For a given l we have therefore to count the number of possible configurations which fulfill $\mathbf{l}=\mathbf{l}_1+\mathbf{l}_3$.

In Table I we have listed this number N for different values l_1 and l_3. Here we have assumed that $2l>l_m$. The sum of all values gives

$$F_1(l_mf_1l)=\sum_{\lambda=0}^{l}(2\lambda+1)-\sum_{\lambda=1}^{l_m-l}\lambda+(2l+1)(l_m-l)-\sum_{\lambda=(l_m-l)-1}^{l}\lambda=-\tfrac{3}{2}l^2+\tfrac{1}{2}l+1+l_m(2l+1). \tag{40}$$

In Table II we have listed similarly all possibilities for l_1 and l_3 for the case $2l<l_m$. Again we can sum up all values and get

$$\bar{F}_1(l_mf_1l)=\sum_{\lambda=0}^{l}(2\lambda+1)+(2l+1)(l_m-2l)+\sum_{\lambda=l+1}^{2l}\lambda,$$

which gives the same results as (40). Therefore we do not have to distinguish between these two cases. However, we have assumed in both cases that $l\leq l_m$. This is not true for all combinations $\mathbf{l}=\mathbf{l}_2+\mathbf{f}_1$; the angular momentum l can be larger than l_m even though l_2 cannot be greater than l_f and f_1 not greater than l_m.

In Table III we have listed all possibilities for l_1 and l_3 in this case. We find

$$F_2(l_mf_1l)=\sum_{\lambda=1}^{2l_m-l+1}\lambda=2l_m{}^2+3l_m-l_ml+\tfrac{1}{2}l^2-\tfrac{3}{2}l+1. \tag{41}$$

We now can explain the index v in the sum (39): If we sum over l we have to introduce either F_1 or F_2 depend-

TABLE I. $2l>l_m$. The number N gives the number of nonvanishing Δ's in (39b) for given l, l_1, l_3. The sum of all these values N gives $F_1(l_mf_1l)$.

l_1	l_3	N
0	l	1
1	$l+1, l, l-1$	3
2	$l+2\cdots l-2$	5
⋮	⋮	⋮
l_m-l	$l_m\cdots(2l_m-l)$	$2(l_m-l)+1$
⋮	⋮	⋮
l	$l_m\cdots0$	$(2l+1)-(l_m-1)$
$l+1$	$l_m\cdots1$	$(2l+1)-(l_m-1)-1$
⋮	⋮	⋮
$l+(l_m-l)$	$l_m\cdots(l_m-l)$	$(2l+1)-l$

TABLE II. $2l<l_m$. The same as in Table I, but with the assumption that $2l<l_m$.

l_1	l_3	N
0	l	1
1	$l+1, l, l-1$	3
⋮	⋮	⋮
l	$2l\cdots0$	$2l+1$
$l+1$	$2l+1\cdots1$	$2l+1$
⋮	⋮	⋮
l_m-l	$l_m\cdots l_m-2l$	$2l+1$
l_m-l+1	$l_m\cdots l_m-2l+1$	$2l$
⋮	⋮	⋮
l_m	$l_m\cdots l_m-l$	$l+1$

TABLE III. The combinations l_1, l_3 which fulfill the triangular rule in the case $l>l_m$. The sum of all the values is called $F_2(l_m,f,l)$.

l_1	l_3	N
0		0
1		0
.		.
.		.
.		0
$l-l_m$	l_m	1
$l-l_m+1$	l_m, l_m-1	2
⋮	⋮	⋮
l_m	$l_m\cdots l-l_m$	$l_m-(l-l_m)+1$

ing on whether $l<l_m$ or $l>l_m$. Having explicitly established the quantities F_1 and F_2, we can now proceed to calculate the double sum in (39). We have to distinguish two cases: $l_f>f_1$ and $l_f<f_1$; i.e., the particle of the particle-hole configuration can have an angular momentum larger or smaller than the Fermi angular momentum. We study here the second case, but note later the results for the first case.

In Table IV the possible values of l are listed for $0\leq l_2\leq l_f$. The sum (39) can now be performed over the values l of the left area in Table IV and yields

$$\sum_{l_1 l_2 l_3}\Delta(l_1 l_2 l_3 f_1)$$
$$=2\sum_{v=0}^{l_f}\sum_{l=f_1-v}^{l_m}F_1(l_m f_1 l)+\sum_{\tau=l_m+1}^{f_1+l_f}\sum_{l=l_m+1}^{\tau}F_2(l_m f_1 l)$$
$$-\sum_{v=1}^{l_m-(f_1-l_f)}\sum_{l=l_m-v+1}^{l_m}F_1(l_m f_1 l)-\sum_{l=f_1-l_f}^{l_m}F_1(l_m f_1 l). \quad (42)$$

It is straightforward to perform this double summation using (40) and (41) and the following relations

$$\sum_0^N \nu^2=\tfrac{1}{3}N^3+\tfrac{1}{2}N^2+\tfrac{1}{6}N,$$
$$\sum_0^N \nu^3=\tfrac{1}{4}N^4+\tfrac{1}{2}N^3+\tfrac{1}{4}N^2. \quad (43)$$

The result for the number of states is [See Eq. (37) and the remarks after Eq. (7). We add a factor $\frac{1}{2}$ to compensate for having counted the states twice.]

$$N(E)=(KR/\pi)^3\tfrac{1}{2}[P(E/E_f)+Q(E/E_f)^2+\cdots]$$
$$\times[A_4(f_1 l_f)l_m^4+A_3(f_1 l_f)l_m^3+A_2(f_1 l_f)l_m^2$$
$$+A_1(f_1 l_f)l_m+A_0(f_1 l_f)], \quad (44)$$

where the $A_v(f_1 l_1)$ are complicated expressions. They are listed in Appendix C. The case $l_f>f_1$ leads to a similar result; only the coefficients A_v are somewhat changed. They are also given in Appendix C.

If we apply (44) to the special case of Pb^{208} where $l_f\approx 4$, $f_1=5$ we obtain

$$N(E)=(1/48)(KR/\pi)^3[P(E/E_f)+Q(E/E_f)^2+\cdots]$$
$$\times[4l_m^4-136l_m^3+2204l_m^2-7727l_m+20117]. \quad (45)$$

With $KR/\pi\approx 3$, $E/E_f=\frac{1}{5}$, $l_m=5$ and multiplying (45) with a factor 2^3 coming from the spin, a factor 2 coming from isospin, and a factor $\frac{1}{2}$ coming from conservation of parity, we find with $\beta\approx\frac{1}{10}$; $\alpha\approx\beta$

$$\bar{N}(E)=N(E)\times 2^3=55\times 8, \quad (45a)$$

for the number of states contributing to process (a) and (b). For the processes (c) and (d) the number of final states is smaller, at least for not too high excitation energies, because there are two holes and one particle in the final configuration. Compared to processes (a) and (b), the two holes below the Fermi surface have fewer possibilities to combine to the right energy and angular momentum. In order to obtain the density of states we have to divide $N(E)$ by the energy interval over which the states are distributed. This interval in our model is the distance between the shells, ΔE. Putting $\Delta E\approx 10$ MeV we thus have

$$\rho(E)=\bar{N}(E)/\Delta E\approx 45 \text{ states/MeV},$$

i.e., a total of about 200 states is available from the processes (a) and (b) within the narrowest observed giant-resonance peak whose width is $\Gamma\approx 2.3$ MeV.[13]

V. CALCULATION OF THE AVERAGED SQUARED MATRIX ELEMENT

We determine the averaged squared matrix element by explicit calculation. We again employ the simplified infinite square-well model used in the previous section. The formula for the level density was general within the accuracy of the model. Now we shall specify to the case $Z=82$, and furthermore, shall only calculate the matrix elements for the protons and for process (a). By calculating all matrix elements of this process we believe

TABLE IV. If $f_1>l_f$ the index l of the sum (39) runs over the values listed below to the left of the vertical dividing line after $l_2=l_f$. The area to the right of the dividing line is added and subtracted again in the summation procedure for reasons of simplicity.

$l_2=$ 0	1	2	$\cdots$ l_m-f_1 $\cdots$	l_f	$\cdots$	$\cdots\cdots$
f_1	f_1+1	f_1+2	l_m	f_1+l_f		
	f_1	f_1+1	l_m+1	⋮		
	f_1-1	f_1	⋮			
		⋮				
				l_m		
				⋮		
					l_m	
					⋮	
				f_1-l_f	f_1-l_f+1 $\cdots$	l_m

[13] E. G. Fuller and E. Hayward, Nucl. Phys. **30**, 613 (1962).

that we do not prejudice our result towards the "most important contribution" but obtain a good average value. From Fig. 7 we find the Fermi momentum $K_pR/\pi \approx 3$. From Eq. (23) we find the "angular momentum of the Fermi surface" to be $l=4$. The Fermi energy is

$$\hbar^2 K_p^2/2M \approx 36.8 \text{ MeV}.$$

In Fig. 8 we give the level scheme for the proton states of Pb^{208} in our square-well model. The giant resonance is created by lifting particles from the closed shell with $l=4$ to the level $l=5$ above the Fermi surface. The shell separation is here $\Delta E \approx 13.2$ MeV.

In Table V we have listed all configurations contributing to process (a), i.e., matrix element (13). The allowed configurations are given by the angular-momentum and parity selection rules contained in the vector coupling coefficients of (13) which fulfill the energy conservation law, i.e., for this process

$$(\hbar^2/2M)(k_1^2+k_3^2-k_2^2-k_4^2)=E=13.2 \text{ MeV}$$

or (46)

$$(\hbar^2/2M)(k_1^2+k_3^2-k_2^2)=E+(\hbar^2/2M)k_4^2=50.0 \text{ MeV}.$$

Note that we have not included the collective energy shift in (46). We are here interested solely in finding explicitly the radial integrals. For this the energy shift is unessential.

It is worth noting, that we obtain from Table V 59 as the number of levels contributing to process (a) while formula (45) gives about 55 (without spin factors). So we find with both counting methods essentially the same numbers.

In the same way as in Table V one can count the numbers of states contributing to process (c) and (d) where the one hole $f_2=4$ is fixed for the matrix element and the holes l_4, l_2 and the particle l_3 can vary. The analog relation to (46) is in this case

$$(\hbar^2/2M)(k_3^2-k_2^2-k_4^2) = E+(\hbar^2/2M)k_4^2 = -36.8 \text{ MeV}. \quad (47)$$

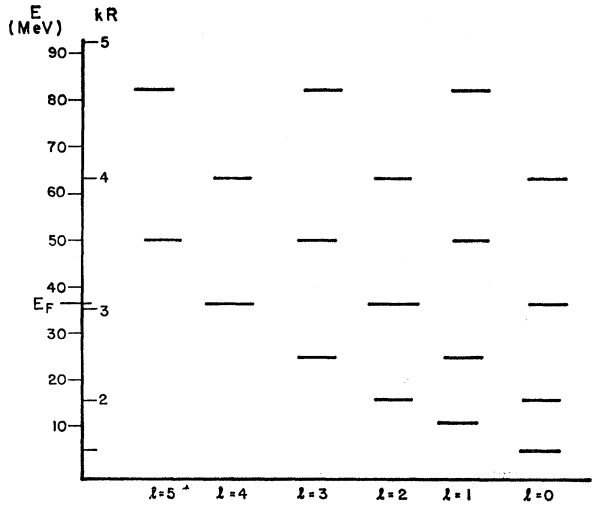

FIG. 8. Level scheme of the asymptotic square-well model.

TABLE V. States contributing to matrix element (a). It is assumed that the degenerate 36.8-MeV states (Table V) are not completely filled, so that two particles can still be there. Furthermore, states with $(K_3R/\pi)=3$, $(K_2R/\pi)=2.5$, $(K_1R/\pi)=3$ fulfill Eq. (46) only approximately. A, listed below, gives 96 states. However, when one subtracts the number of states which appear a second time, albeit in a different coupling scheme, one obtains 59 for the number of final states (without spin factors) contributing to process (a).

f_1	l_3	l_2	l_1	A	K_3R/π	K_2R/π	K_1R/π
5	5	4	4	8, 6, 4, 2	$\frac{7}{2}$	3	3
5	5	4	2	6, 4, 2	$\frac{7}{2}$	3	3
5	5	4	0	4	$\frac{7}{2}$	3	3
5	5	2	4	6, 4, 2	$\frac{7}{2}$	3	3
5	5	2	2	4, 2	$\frac{7}{2}$	3	3
5	5	2	0	2	$\frac{7}{2}$	3	3
5	5	0	4	4	$\frac{7}{2}$	3	3
5	5	0	2	2	$\frac{7}{2}$	3	3
5	4	4	5	9, 7, 5, 4, 1	3	3	$\frac{7}{2}$
5	4	4	3	7, 5, 3, 1	3	3	$\frac{7}{2}$
5	4	4	1	5, 3	3	3	$\frac{7}{2}$
5	4	3	0	3	3	$\frac{5}{2}$	3
5	4	2	5	7, 5, 3	3	3	$\frac{7}{2}$
5	4	2	3	5, 3, 1	3	3	$\frac{7}{2}$
5	4	1	4	5, 3	3	$\frac{5}{2}$	3
5	4	1	2	3, 1	3	$\frac{5}{2}$	3
5	4	1	0	1	3	$\frac{5}{2}$	3
5	4	0	5	5	3	3	$\frac{7}{2}$
5	4	0	3	3	3	3	$\frac{7}{2}$
5	4	0	1	1	3	3	$\frac{7}{2}$
5	3	4	4	8, 6, 4, 2	$\frac{7}{2}$	3	3
5	3	4	2	6, 4, 2	$\frac{7}{2}$	3	3
5	3	4	0	4	$\frac{7}{2}$	3	3
5	3	2	4	8, 6, 4, 2	$\frac{7}{2}$	3	3
5	3	2	2	4, 2	$\frac{7}{2}$	3	3
5	3	2	0	2	$\frac{7}{2}$	3	3
5	3	0	4	4	$\frac{7}{2}$	3	3
5	3	0	2	2	$\frac{7}{2}$	3	3
5	2	4	5	7, 5, 3	3	3	$\frac{7}{2}$
5	2	4	3	7, 5, 3	3	3	$\frac{7}{2}$
5	2	4	1	7, 5, 3	3	3	$\frac{7}{2}$
5	2	3	4	7, 5, 3	3	$\frac{5}{2}$	3
5	2	3	2	5, 3	3	$\frac{5}{2}$	3
5	2	3	0	3	3	$\frac{5}{2}$	3
5	2	2	1	3	3	3	$\frac{7}{2}$
5	2	1	4	5, 3	3	$\frac{5}{2}$	3
5	2	1	2	3	3	$\frac{5}{2}$	3
5	2	0	5	5	3	3	$\frac{7}{2}$
5	2	0	3	3	3	3	$\frac{7}{2}$
5	1	4	4	6, 4	$\frac{7}{2}$	3	3
5	1	4	2	6, 4	$\frac{7}{2}$	3	3
5	1	4	0	4	$\frac{7}{2}$	3	3
5	1	2	4	6, 4	$\frac{7}{2}$	3	3
5	1	2	2	4	$\frac{7}{2}$	3	3
5	1	0	4	4	$\frac{7}{2}$	3	3
5	0	4	5	5	3	3	$\frac{7}{2}$
5	0	4	3	5	3	3	$\frac{7}{2}$
5	0	4	1	5	3	$\frac{5}{2}$	3
5	0	3	2	5	3	$\frac{5}{2}$	3
5	0	2	5	5	3	3	$\frac{7}{2}$
5	0	2	3	5	3	3	$\frac{7}{2}$
5	0	1	4	5	3	$\frac{5}{2}$	3
5	0	0	5	5	3	3	$\frac{7}{2}$

TABLE VI. The possible configurations contributing to processes (c) and (d). The assumptions are the same as in Table V. The number of nonrepeating states is here only 25 compared to 59 in the former case. There are 37 states when one includes the states in different coupling schemes.

f_2	l_3	l_2	l_4	A	k_3R/π	k_2R/π	K_4R/π
4	4	4	4	8, 6, 4, 2	3	3	3
4	4	4	2	6, 4, 2	3	3	3
4	4	4	0	4	3	3	3
4	4	2	4	6, 4, 2	3	3	3
4	4	2	2	4, 2	3	3	3
4	4	2	0	2	3	3	3
4	4	0	4	4	3	3	3
4	4	0	2	2	3	3	3
4	2	4	4	6, 4, 2	3	3	3
4	2	4	2	6, 4, 2	3	3	3
4	2	4	2	4	3	3	3
4	2	2	4	6, 4, 2	3	3	3
4	2	2	2	4, 2	3	3	3
4	2	2	0	2	3	3	3
4	2	0	4	4	3	3	3
4	2	0	2	2	3	3	3
4	0	4	4	4	3	3	3
4	0	4	2	4	3	3	3
4	0	4	0	4	3	3	3
4	0	2	4	4	3	3	3
4	0	2	2	4	3	3	3
4	0	0	4	4	3	3	3
				37			

Table VI gives a list of the possible states for the processes (c) and (d). Under the same assumptions as for Table V we find about 25 states (without the spin factors) contributing to (c) and (d) while 59 states contributed to (a) and (b).

The radial integrals for the different configurations of Table V were calculated by using the asymptotic expressions for the spherical Bessel functions, except for the one with the highest l value, which here is $l=5$. The latter we approximated by

$$j_l(kr)=c_l(kr)^l[1-(r/R)^l]. \tag{48}$$

The normalization factor is

$$c_l=\frac{k^{3/2}}{(kR)^{l+3/2}}\left[\frac{(2l+3)(3l+3)(4l+3)}{2l^2}\right]^{1/2}. \tag{49}$$

This leads to elementary integrals of the type

$$\int r^\alpha \cos k_1 r \cos k_2 r \cos k_3 r dr.$$

We have calculated all the squares of the matrix elements of the states listed in Table V and averaged them. The result is

$$(|\langle\Psi_u|V^{(a)}|\Psi_v\rangle|^2)_{\rm av}=(V_0/4\pi R^3)^2\times 0.085, \tag{50}$$

where V_0 is the strength of the δ-force potential.

VI. DISCUSSION AND RESULTS

Inserting (50) and (45) in (19) we find

$$\Gamma=(1/48)(KR/\pi)^3[P(E/E_f)+Q(E/E_f)^2+\cdots]\times[4l_m^4-136l_m^3+2204l_m^2-7727l_m+20117]\times 0.085(V_0/4\pi R^3)^2\times 2\pi\times 2^3\times(G/\Delta E). \tag{51}$$

Really l_m is a function of E via the relation (23). So the energy dependence of the width is contained in the second and third factor. The factor 2^3 comes from the spin while a factor 2 from the isospin and a factor $\frac{1}{2}$ from parity cancel each other. The factor G takes into account the other graphs: If we put the contributions of graphs (a) and (b) equal and those of graphs (c) and (d) roughly $\frac{1}{3}$ of the contributions of (a), we have $G=8/3$. The reason for putting the contributions of (c) and (d) to be $\frac{1}{3}$ of the contributions of (a) is the fact that the number of states contributing to (c) and (d) is roughly $\frac{1}{3}$ of the number of states contributing to (a). (See the preceding section, especially Tables V and VI.) We thus imply that the average matrix element is the same for both classes of graphs. If we write for the energy dependence

$$\Gamma=\Gamma_0 E^g \tag{52}$$

as we did in an earlier paper,[14] formula (51) gives us for the exponent g the value $g=1.8$ if E varies between 10 and 15 MeV and l_m is assumed to grow from $l_m=5$ to $l_m=6$ in this energy region. This is in reasonable agreement with experimental observation: $g_{\rm exp}\approx 2.0$.[15]

The absolute value of the width depends strongly on the strength V_0 of the potential. In different particle-hole calculations for light nuclei this strength varies quite a bit,[16,17]

$$\frac{V_0}{4\pi R^3}=\left\{\begin{matrix}4.5\\9.2\end{matrix}\right\}\frac{1}{(\alpha R)^3}\ \text{MeV}\quad \alpha=0.54\ \text{F}^{-1}\ \text{for Ca}^{40}, \tag{53}$$

where $R\approx 7.2$ F for lead. The best value of the potential lies close to the highest value of (53), i.e., near 9 MeV. Choosing again $\beta=\frac{1}{10}$, $E/E_f\approx\frac{1}{4}$, we find

$$\Gamma=\left\{\begin{matrix}0.42\\2.25\end{matrix}\right\}\ \text{MeV} \tag{54}$$

for the limiting values of V_0 given in (53). The largest uncertainty in this result is due to the strength of the interactions, V_0, since it enters quadratically. The uncertainty in the value of the mean-squared matrix element Eq. (50) is probably not worse than a factor 1.5; a similar uncertainty is probably associated with the quantities α and β, (34) and (36). These uncer-

[14] M. Danos and W. Greiner, Phys. Letters 8, 113 (1964).
[15] E. Ambler, E. G. Fuller, and H. Marshak, Phys. Rev. 138, B117 (1965).
[16] V. Gillet, Nucl. Phys. 51, 410 (1964).
[17] L. G. Weigert and J. M. Eisenberg (to be published).

tainties, however, enter only the absolute magnitude of the width.

To summarize, we have shown that the thermalization process indeed is sufficient to give the total width of the giant resonance. The contribution of the direct emission of fast particles to the width thus can have a magnitude consistent with the Courant process[11] and no further damping mechanisms are needed. The computed width has a magnitude and energy dependence in agreement with the experiment.

APPENDIX A

We would like to derive formula (19) by two methods. First, in this Appendix A, we shall use time-dependent perturbation theory since this method is simple and transparent, and all the essential points can be illustrated in the derivation. In Appendix B, we shall use a method which is of lowest order in the electromagnetic interaction, but is formally exact in the nuclear interactions. This will allow to state precisely the random-phase assumption discussed in the Introduction, i.e., the quality of the approximation implicit in the treatment, and elaborated on below. With this method we will show that Eq. (19) is more generally valid than its form implies. We will furthermore show that the photon-absorption cross section is a superposition of Lorentz lines rather than Breit-Wigner lines; i.e., the line shape coincides with the classical line shape.

According to the Introduction, our initial conditions are a collective state which has been generated as the result of the absorption of a photon. In order to apply time-dependent perturbation theory we have to define the two-particle–two-hole states into which the collective state decays. Let us denote them by $\Phi_\alpha{}^{(2)}$. They are themselves broadened by continuum states ψ. We describe this broadening following the treatment of Fano.[18] We thus write:

$$\Psi_\alpha{}^{(2)}(E)=a_\alpha(E)\Phi_\alpha{}^{(2)}+\int dE' b_\alpha(E,E')\psi(E'). \quad \text{(A1)}$$

According to the Introduction the continuum states ψ are mostly rather complicated states and the matrix element between the collective state $\Phi^{(1)}$ and ψ vanishes. The diverse normalizations and matrix elements are

$$\langle\Phi^{(1)},H\Phi^{(1)}\rangle=E_0, \quad \text{(A2)}$$

$$\langle\Phi_{\alpha'}{}^{(2)},H\Phi_\alpha{}^{(2)}\rangle=E_\alpha\delta_{\alpha'\alpha}, \quad \text{(A3)}$$

$$\langle\Phi_\alpha{}^{(2)},H\Phi^{(1)}\rangle=V_\alpha, \quad \text{(A4)}$$

$$\langle\Phi^{(1)},H\psi\rangle=0, \quad \text{(A5)}$$

$$\langle\Phi_\alpha{}^{(2)},H\psi(E)\rangle=W_\alpha(E), \quad \text{(A6)}$$

$$\langle\Psi_{\alpha'}{}^{(2)}(E'),H\Psi_\alpha{}^{(2)}(E)\rangle=E\delta_{\alpha'\alpha}\delta(E-E'), \quad \text{(A7)}$$

$$\langle\Psi_{\alpha'}{}^{(2)}(E'),\Psi_\alpha{}^{(2)}(E)\rangle=\delta_{\alpha'\alpha}\delta(E-E'), \quad \text{(A8)}$$

[18] U. Fano, Phys. Rev. **124**, 1866 (1961).

and, according to Fano[18] there holds

$$|a_\alpha(E)|^2=\frac{|W_\alpha(E)|^2}{[E-E_\alpha-F_\alpha(E)]^2+\pi^2|W_\alpha(E)|^4}, \quad \text{(A9)}$$

with

$$F_\alpha(E)=P\int dE'\frac{|W_\alpha(E')|^2}{E-E'}. \quad \text{(A10)}$$

We now solve the Schrödinger equation

$$\frac{\hbar}{i}\frac{\partial}{\partial t}\Psi=H\Psi \quad \text{(A11)}$$

by the ansatz

$$\Psi=A(t)\Phi^{(1)}e^{-i(E_0/\hbar)t}+\sum_\alpha\int dE' B_\alpha(E',t)\Psi_\alpha{}^{(2)}(E')e^{-i(E'/\hbar)t}, \quad \text{(A12)}$$

with the boundary condition

$$\begin{aligned}A(0)&=1,\\ B(E,0)&=0,\end{aligned} \quad \text{(A13)}$$

which yields in the well-known manner,[19] using the relations (A2)–(A8), the set of differential equations

$$-(\hbar/i)B_\alpha(E)e^{-i(E/\hbar)t}=a_\alpha(E)V_\alpha e^{-i(E_0/\hbar)t}. \quad \text{(A14)}$$

Thus, we finally obtain for the probability per unit time of transitions into any of the states $\Psi_\alpha{}^{(2)}$ the equation

$$T=\frac{d}{dt}\int dE|B_\alpha(E)|^2=\sum_\alpha\frac{2\pi}{\hbar}|V_\alpha|^2|a_\alpha(E_0)|^2=\sum_\alpha\frac{2\pi}{\hbar}|V_\alpha|^2\frac{\gamma_\alpha/2\pi}{(E_0-\epsilon_\alpha)^2+\gamma_\alpha{}^2/4}, \quad \text{(A15)}$$

where we have used (A9) and have introduced obvious abbreviations. Lastly, we assume that the energies ϵ_α are distributed at random with a density $\rho^{(E)}$, and that the matrix elements $|V_\alpha|^2$ also form a random distribution. Then one can remove an average matrix element $(|V|^2)_{\text{av}}$ from the sum and replace the summation over α by an integration over ϵ. This way one obtains

$$\Gamma=\hbar T=2\pi(|V|^2)_{\text{av}}\rho(E_0), \quad \text{(A16)}$$

which is Eq. (19) of the text. This formula is valid as long as $\gamma\rho\gg1$ and is then independent of γ. In the present case, $\gamma\rho\approx$ 50–100, since the damping of two-particle–two-hole states by three-particle–three-hole states will be of the same order of magnitude as the damping of particle-hole states by two-particle–two-hole states.

[19] L. I. Schiff, *Quantum Mechanics* (McGraw-Hill Book Company, Inc., New York, 1955), Chap. VIII.

APPENDIX B

In this Appendix we shall use a stationary-state description to derive Eq. (19) and to discuss the line shape of the photon-absorption cross sections. The starting point is the optical theorem

$$\sigma=(4\pi/k)\ \mathrm{Im}\tilde{f}(E,0) \tag{B1}$$

and the scattering amplitude is, except for constants, a matrix element of the operator

$$f=-\boldsymbol{\varepsilon}_2\cdot\mathbf{D}[(E-H+i\eta)^{-1}-(E+H+i\eta)^{-1}]\boldsymbol{\varepsilon}_1\cdot\mathbf{D}, \tag{B2}$$

$\eta\rightarrow 0$.

Here $\mathbf{D}$ is the dipole operator and $\boldsymbol{\varepsilon}_2$ and $\boldsymbol{\varepsilon}_1$ are the polarizations of the outgoing and incoming photon, respectively. For elastic forward scattering, $\boldsymbol{\varepsilon}_1=\boldsymbol{\varepsilon}_2$; η is an infinitesimal positive number which determines the boundary conditions.[20] If, instead, one puts $\eta=\Gamma/2$, one obtains immediately a Lorentz shape. This procedure is, however, *ad hoc*, even though practiced quite widely. The Lorentz, instead of the Breit-Wigner shape results from the presence of the second energy denominator which has its origin in the crossed Feynman diagram in which a photon is emitted before the incoming photon has been absorbed.

In order to evaluate the matrix elements we have to define the nuclear states. For reasons of simplicity we assume that the collective particle-hole state contains only bound particle states, i.e., states whose wave function vanishes as $r\rightarrow\infty$. This assumption may even be fulfilled in heavy nuclei, the shell separation being of the order of the binding energy. The direct emission then results from the Auger effect, a process sometimes called "autoionization." As stated in the Introduction we shall neglect this contribution to the damping. It has been treated, e.g., by Fano.[18] We are going to utilize Fano's formulation in our derivations.

The nuclear wave function is expanded in the complete set of states

$$\psi(E)=\sum_\alpha A_\alpha^{(1)}(E)\varphi_\alpha^{(1)}+\sum_\beta A_\beta^{(2)}(E)\varphi_\beta^{(2)}+\cdots$$
$$+\sum_\gamma\int B_\gamma^{(1)}(E,E')\psi_\gamma^{(1)}(E')dE'$$
$$+\sum_\delta\int B_\delta^{(2)}(E,E')\psi_\delta^{(2)}(E')dE'+\cdots, \tag{B3}$$

where the states $\varphi_\alpha^{(1)}$, $\varphi_\beta^{(2)},\cdots$ denote bound particle-hole, two-particle–two-hole, etc. states while $\psi^{(1)}(E)$, $\psi^{(2)}(E)\cdots$ are similar unbound states. According to Fano's prescription one has to begin by diagonalizing the different categories of states, separately. We thus have to diagonalize, e.g., the particle-hole states separately, which is the usual procedure. Let us call the diagonalized states $\Phi_\alpha^{(n)}$. They thus fulfill

$$\langle\Phi_{\alpha'}^{(n)},H\Phi_\alpha^{(n)}\rangle=E_\alpha^{(n)}\delta_{\alpha\alpha'};$$
$$\langle\Phi_{\alpha'}^{(n')},\Phi_\alpha^{(n)}\rangle=\delta_{\alpha\alpha'}\delta_{nn'}. \tag{B4}$$

However,

$$\langle\Phi_{\alpha'}^{(n')},H\Phi_\alpha^{(n)}\rangle=H_{\alpha'\alpha}^{(n',n)}\neq 0,\quad n'\neq n \tag{B5}$$

but, owing to the two-body character of the forces, only those off-diagonal elements do not vanish where $n'=n\pm 1$.

We now turn to the continuum states. According to Fano[18] they also have to be diagonalized. We call them $\Psi_\gamma^{(n)}(E)$. Further, they are to be normalized as

$$\langle\Psi_{\gamma'}^{(n)}(E'),H\Psi_\gamma^{(n)}(E)\rangle=E\delta(E'-E)\delta_{\gamma'\gamma}, \tag{B6}$$

$$\langle\Psi_{\gamma'}^{(n')}(E'),\Psi_\gamma^{(n)}(E)\rangle=\delta(E'-E)\delta_{\gamma'\gamma}\delta_{n'n}. \tag{B7}$$

Again, the elements

$$V_{\gamma'\gamma}^{(n',n)}(E',E)\equiv\langle\Psi_{\gamma'}^{(n')}(E'),H\Psi_\gamma^{(n)}(E)\rangle \tag{B8}$$

in general do not vanish for $n'=n\pm 1$. Finally, the off-diagonal elements

$$W_{\alpha\gamma}^{(n',n)}(E)\equiv\langle\Phi_\alpha^{(n')},H\Psi_\gamma^{(n)}(E)\rangle \tag{B9}$$

also exist. However, they also do not vanish only for $n'=n$, $n\pm 1$. The energy matrix thus now has the form shown in Fig. 9.

Fano's procedure would now require the diagonalization of all bound states and all continuum states separately, and then, at the end, the mixing of the discrete and the continuum states. However, we shall follow a slightly different procedure. We begin by mixing the discrete and the continuum states at the highest n, and write

$$\chi_{\alpha'}^{(n)}(E)=\sum_\alpha a_{\alpha'\alpha}^{(n)}(E)\Phi_\alpha^{(n)}$$
$$+\int dE'\sum_\gamma b_{\alpha'\gamma}^{(n)}(E,E')\Psi_\gamma^{(n)}(E'). \tag{B10}$$

At this point we want to simplify the treatment somewhat. We invoke the random-phase assumption to separate the different discrete states. The meaning of it is the following. The Hamiltonian is diagonal in the states $\Phi_\alpha^{(n)}$. These states can, however, still mix via the continuum states $\Psi_\gamma^{(n)}$. We are going to neglect this mixing with the justification that the different continua will contribute with random matrix elements to the mixing, thus leading mainly to damping of the states. Then one can separate (B10) into a set of independent equations

$$\chi_\alpha^{(n)}(E)=\tilde{a}_\alpha^{(n)}(E)\Phi_\alpha^{(n)}$$
$$+\int\sum_\gamma\tilde{b}_{\alpha\gamma}^{(n)}(E')\Psi_\gamma^{(n)}(E')dE'. \tag{B11}$$

[20] B. A. Lippmann and J. Schwinger, Phys. Rev. **79**, 469 (1950)

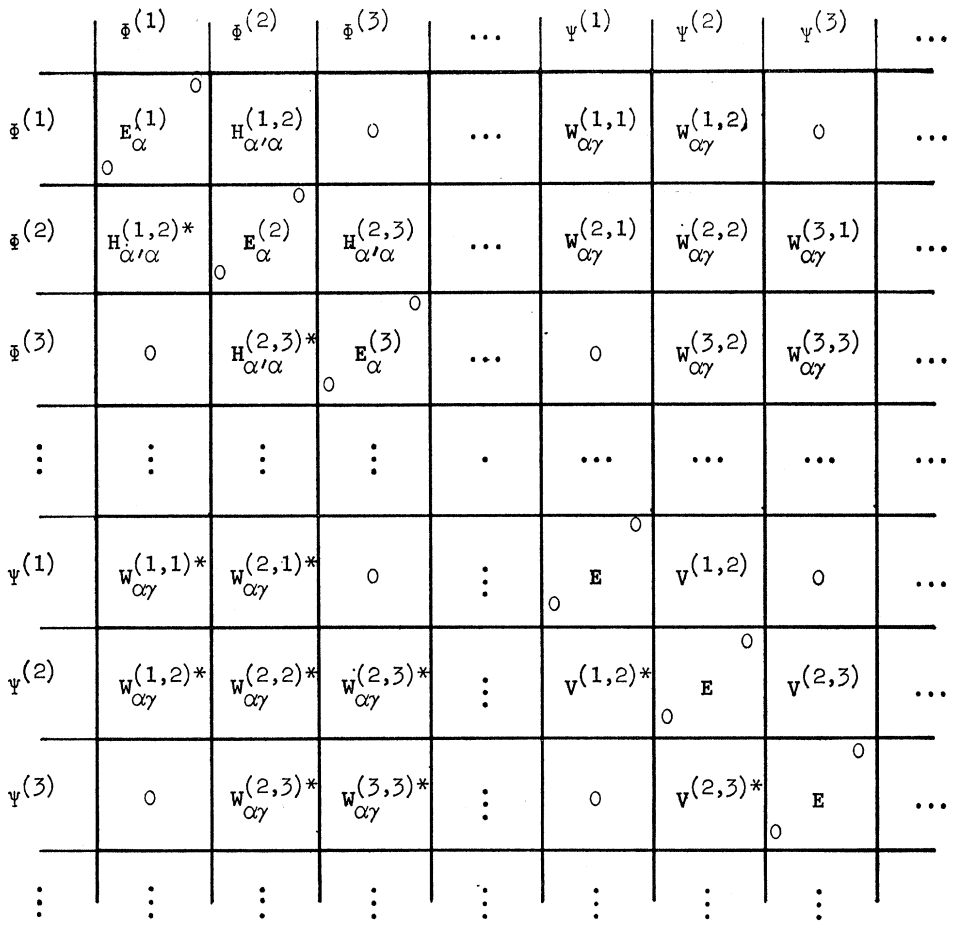

FIG. 9. Form of the energy matrix.

The appearance of several continua in (B11) leads to to no complications.[18] Explicit expressions for $\tilde{a}$ and $\tilde{b}$ are given in Fano's paper. We quote

$$|\tilde{a}_\alpha{}^{(n)}(E)|^2 = \frac{|U_\alpha{}^{(n)}(E)|^2}{[E-E_\alpha{}^{(n)}-G_\alpha{}^{(n)}(E)]^2+\pi^2|U_\alpha{}^{(n)}(E)|^4}, \quad \text{(B12)}$$

where

$$|U_\alpha{}^{(n)}(E)|^2=\sum_\gamma|W_{\alpha\gamma}{}^{(n,n)}(E)|^2 \quad \text{(B13)}$$

and

$$G_\alpha{}^{(n)}(E)=P\int dE'\frac{|U_\alpha{}^{(n)}(E)|^2}{E-E'}. \quad \text{(B14)}$$

The functions $\chi_\alpha{}^{(n)}(E')$ then are normalized as

$$\langle\chi_\alpha{}^{(n)}(E'),\chi_\alpha{}^{(n)}(E)\rangle=\delta(E-E'), \quad \text{(B15)}$$

i.e., they have the character of continuum states.

We now proceed to the next lower n; let us call it for the time being $n-1$. We again write the equation analogous to (B10). It now has the same form except that in addition to the continua $\Psi_\gamma{}^{(n-1)}$ there appear also the continuum states $\chi_\alpha{}^{(n)}$. We again invoke the random-phase argument to separate the equations, i.e., go to the form analogous to (B11). At this time, the random-phase argument has improved in quality: There are more continuum states available than in the previous step. Thus the equations have the form

$$\chi_\alpha{}^{(n-1)}(E)=\tilde{a}_\alpha{}^{(n-1)}(E)\Phi_\alpha{}^{(n-1)} + \int[\textstyle\sum_\gamma \bar{b}_{\alpha\gamma}{}^{(n-1)}(E')\Psi_\gamma{}^{(n-1)}(E') + \sum_{\alpha'}\bar{c}_{\alpha\alpha'}{}^{(n-1)}(E')\chi_{\alpha'}{}^{(n)}(E')]dE'. \quad \text{(B16)}$$

The bar on $\bar{b}$ and $\bar{c}$ indicates that the necessary diagonalization has been performed so that the off-diagonal elements (B8) cancel. Then again (B12) holds, except that (B13) and (B14) have to be augmented with the contributions from χ: In (B12) U and G have to be replaced by $\bar{U}$ and $\bar{G}$ which are given by

$$|\bar{U}_\alpha{}^{(n-1)}(E)|^2=\sum_\gamma|W_{\alpha\gamma}{}^{(n-1,n-1)}(E)|^2 + \sum_{\alpha'}|T_{\alpha\alpha'}{}^{(n-1,n)}(E)|^2, \quad \text{(B17)}$$

$$\bar{G}_\alpha{}^{(n-1)}(E)=P\int dE'\frac{|\bar{U}_\alpha{}^{(n-1)}(E')|^2}{E-E'}, \quad \text{(B18)}$$

and where

$$T_{\alpha\alpha'}{}^{(n-1,n)}(E)=\langle\Phi_\alpha{}^{(n-1)},H\chi_{\alpha'}{}^{(n)}(E)\rangle. \quad \text{(B19)}$$

These equations now allow a recursion in n down to $n=1$. They remain unchanged in form since no matrix elements exist connecting functions with n differing by more than one. The random-phase argument improves the further down one proceeds on the n ladder. The errors resulting from the marginal applicability of the argument at the highest n at the beginning of the procedure get attenuated: The contributions of the W-matrix elements in (B17) tend to overshadow the contributions of the T-matrix elements. This is a cumulative effect in going through the recurrence procedure.

We now can return to (B2). Only particle-hole states have finite dipole matrix elements to the ground state. Therefore (B2) becomes

$$\langle 0|f(E,0)|0\rangle=\sum_\alpha\int dE'\langle 0|\boldsymbol{\varepsilon}\cdot\mathbf{D}|\chi_\alpha{}^{(1)}(E')\rangle \times[-(E-E'+i\eta)^{-1}+(E+E'+i\eta)^{-1}] \times\langle\chi_\alpha{}^{(1)}(E')|\boldsymbol{\varepsilon}\cdot\mathbf{D}|0\rangle. \quad \text{(B20)}$$

Since we are interested in the imaginary part of f we need only the δ-function part of the relation $-(E-E'+i\eta)^{-1}=-P(E-E')^{-1}+i\pi\delta(E-E')$. Furthermore, we disregard the nonresonating "direct" transisitions involving the "continuum" contributions to $\chi_\alpha{}^{(1)}$, the integral in (B11), as discussed in the Introduction. We thus obtain

$$\mathrm{Im}\langle 0|f(E,0)|0\rangle=\sum_\alpha\int_0^\infty dE'|\langle 0|\boldsymbol{\varepsilon}\cdot\mathbf{D}|\Phi_\alpha{}^{(1)}\rangle|^2 \times\pi[\delta(E-E')-\delta(E+E')]|\tilde{a}_\alpha{}^{(1)}(E')|^2. \quad \text{(B21)}$$

According to (B12), $|\tilde{a}_\alpha{}^{(1)}|^2$ has superficially the form of a Breit-Wigner line. However, firstly even (B12) is not a Breit-Wigner line since both the "position" and the "width" of the resonance, i.e., $E_\alpha{}^{(1)}+G_\alpha{}^{(1)}$ and $|U_\alpha{}^{(1)}|^2$, depend on the energy and are not constants as they are in a Breit-Wigner line. Secondly, and more importantly, Imf has poles symmetrical to the imaginary axis in contrast to the Breit-Wigner line: Imf is time-reversal invariant.

We now make the above statements explicit. To that end we perform a meromorphic expansion of $|\tilde{a}_\alpha{}^{(1)}(E)|^2$, the only energy-dependent factor left in the integral. We thus write

$$|\tilde{a}_\alpha{}^{(1)}(E')|^2=\sum_n\frac{R_{\alpha n}\Gamma_{\alpha n}}{(E'-E_{\alpha n})^2+\Gamma_{\alpha n}{}^2/4}+F_\alpha(E'). \quad \text{(B22)}$$

We have explicitly taken into account the reality condition and have assumed that no pole occurs at $E=0$, i.e., we have assumed that the nucleus is part of a neutral atom so that no Thompson scattering takes place. [Naturally, one observes the nuclear Thompson scattering in elastic photon scattering of photons below the (γ,n) threshold since the highest electronic resonance lines lie at very much lower energies. However, at $E=0$ no pole occurs.] In (B22) the residua $R_{\alpha n}$, and the positions of the poles, specified by $E_{\alpha n}$ and $\Gamma_{\alpha n}$, are by definition independent of energy; $F_\alpha(E)$ is an entire function. We now perform the integration over E'. Since we are doing nonrelativistic quantum mechanics the energy E' is restricted to positive values. However, the photon energy E must have both positive and negative values because of the reality of the electromagnetic field. In other words, the photons must be treated relativistically under any circumstances. After all, emission and absorption of photons takes place, and they have rest mass zero. For $E>0$ only the first δ function contributes because of the region of integration, while for $E<0$ only the second δ function makes a contribution. Thus, Imf has as a function of E poles which are symmetric with respect to the imaginary axis, namely

$$\mathrm{Im}\langle 0|f|0\rangle=\sum_\alpha|\langle 0|\boldsymbol{\varepsilon}\cdot\mathbf{D}|\Phi_\alpha{}^{(1)}\rangle|^2|\tilde{a}_\alpha{}^{(1)}(E)|^2 \quad \text{for } E>0$$
$$=-\sum_\alpha|\langle 0|\boldsymbol{\varepsilon}\cdot\mathbf{D}|\Phi_\alpha{}^{(1)}\rangle|^2|\tilde{a}_\alpha{}^{(1)}(-E)|^2 \quad \text{for } E<0. \quad \text{(B23)}$$

Collecting the contribution from the poles when inserting (B22) in (B23), and writing for the "background" part the entire function $B(E)$, we obtain

$$\mathrm{Im}\langle f\rangle=\sum_{\alpha n}\frac{2\pi R_{\alpha n}\Gamma_{\alpha n}EE_{\alpha n}}{(E^2-\epsilon_{\alpha n}{}^2)^2+\Gamma_{\alpha n}{}^2E^2}+B(E), \quad \text{(B24)}$$

where

$$\epsilon_{\alpha n}{}^2=E_{\alpha n}{}^2+\Gamma_{\alpha n}{}^2/4. \quad \text{(B25)}$$

If we consider that the meromorphic expansion (B22) contains just one pole, i.e., if we assume that one can replace the matrix elements (B17) and (B18) in (B12) by constants, we obtain immediately

$$\mathrm{Im}\langle f\rangle=\sum_\alpha\frac{2\pi R_\alpha\Gamma_\alpha EE_\alpha}{(E^2-\epsilon_\alpha{}^2)^2+\Gamma_\alpha{}^2E^2}, \quad \text{(B26)}$$

where

$$\Gamma_\alpha=\sum_\gamma|W_{\alpha\gamma}{}^{(1,1)}(E_\alpha)|^2+\sum_\alpha|T_{\alpha\alpha}{}^{(1,2)}(E_\alpha)|^2. \quad \text{(B27)}$$

The matrix elements (B17) and (B18) are definitely not independent of the energy. They may, however, very well be rather insensitive functions of the energy over the important, but limited, energy region.

One obtains Eq. (19), Sec. III, immediately from (B27) by using (B19), inserting the expression (B12) for $\tilde{a}_\alpha{}^{(2)}(E)$, and performing an average over the energy under the assumption $\Gamma_{\alpha\rho}\gg 1$, as in Appendix A.

APPENDIX C

We note here the explicit expressions for the coefficients A_ν of Eq. (44). The two cases (1) $f_1>l_f$ and (2) $f_1<l_f$ have to be distinguished. The upper value and

sign in the following formulas corresponds to the first case, the lower value and sign to the second.

$$A_4=\tfrac{1}{6},$$

$$A_3=\begin{Bmatrix} l_f \\ f_1 \end{Bmatrix}-(7/6)(l_f+f_1)+\tfrac{1}{2}(\pm l_f\mp f_1+1)^3\mp l_f\pm f_1-\tfrac{2}{3},$$

$$A_2=3\left(\begin{Bmatrix} l_f \\ f_1 \end{Bmatrix}+1\right)+2(l_f+f_1)(2l_f+2f_1-1)\mp l_f\pm f_1-\tfrac{1}{4},$$

$$A_1=-\frac{2}{3}\left(\begin{Bmatrix} l_f \\ f_1 \end{Bmatrix}+1\right)^3+\frac{2}{3}\begin{Bmatrix} l_f \\ f_1 \end{Bmatrix}+(2f_1+1)\begin{Bmatrix} l_f \\ f_1 \end{Bmatrix}\left(\begin{Bmatrix} l_f \\ f_1 \end{Bmatrix}+1\right)$$
$$+2(-f_1^2-f_1+3)\left(\begin{Bmatrix} l_f \\ f_1 \end{Bmatrix}+1\right)-\tfrac{1}{3}(f_1+l_f+1)^3+\tfrac{3}{2}(f_1+l_f)(f_1+l_f+1)+\tfrac{1}{3}(\pm l_f\mp f_1+1)^3$$
$$-\tfrac{3}{4}(\pm l_f\mp f_1+1)^2+(1/18)(\pm l_f\mp f_1)+(\pm f_1-l_f-1)\left(f_1-\begin{Bmatrix} l_f \\ f_1 \end{Bmatrix}\right)-l_f+\begin{Bmatrix} f_1 \\ l_f \end{Bmatrix}-7/12,$$

$$A_0=-\frac{1}{4}\left(\begin{Bmatrix} l_f \\ f_1 \end{Bmatrix}+1\right)^4+\frac{1}{2}\left(\begin{Bmatrix} l_f \\ f_1 \end{Bmatrix}+1\right)^3-\frac{1}{4}\begin{Bmatrix} l_f \\ f_1 \end{Bmatrix}+\tfrac{1}{6}(3l_f-2)\left[2\left(\begin{Bmatrix} l_f \\ f_1 \end{Bmatrix}+1\right)^3-3\begin{Bmatrix} l_f \\ f_1 \end{Bmatrix}^2-5\begin{Bmatrix} l_f \\ f_1 \end{Bmatrix}\right]$$
$$-\tfrac{1}{2}f_1^2+\tfrac{3}{2}f_1+\tfrac{1}{2}(f_1-1)\begin{Bmatrix} l_f \\ f_1 \end{Bmatrix}\left(\begin{Bmatrix} l_f \\ f_1 \end{Bmatrix}+1\right)+(f_1^2-1)(f_1-2)\left(\begin{Bmatrix} l_f \\ f_1 \end{Bmatrix}+1\right)+(1/24)(l_f+f_1+1)^4-\tfrac{1}{4}(l_f+f_1+1)^3$$
$$+\tfrac{2}{3}(l_f+f_1)+(11/24)(l_f+f_1)^2+\tfrac{1}{8}(\pm l_f\mp f_1+1)^4-\tfrac{1}{8}(l_f-f_1)^2-\tfrac{1}{4}(\pm l_f\mp f_1+1)^3+\tfrac{1}{6}(\pm l_f\mp f_1)$$
$$-\frac{1}{3}\left(f_1-\begin{Bmatrix} l_f \\ f_1 \end{Bmatrix}\right)^3+\frac{1}{6}\left(3f_1-3\begin{Bmatrix} l_f \\ f_1 \end{Bmatrix}+8\right)\left(f_1-\begin{Bmatrix} l_f \\ f_1 \end{Bmatrix}-1\right)+\frac{1}{4}\left(f_1-\begin{Bmatrix} l_f \\ f_1 \end{Bmatrix}\right)^3\left(f_1-\begin{Bmatrix} l_f \\ f_1 \end{Bmatrix}-1\right)+(11/8).$$